

# Three-Particle Cumulant versus Three-Particle Jet-Like Correlation

Jason G. Ulery and Fuqiang Wang

Department of Physics, Purdue University  
525 Northwestern Avenue, West Lafayette, Indiana 47907, USA

## Abstract

Two-particle jet-like azimuthal correlations have revealed intriguing modifications to the away side of the high  $p_T$  trigger particle in relativistic heavy-ion collisions. Three-particle jet-like azimuthal correlation and 3-particle azimuthal cumulant have been analyzed in experiments in attempt to distinguish conical emission of jet-like particles from other physics mechanisms. We investigate the difference between 3-particle jet-like correlation and 3-particle cumulant in azimuth. We argue, under the circumstance where the away-side 2-particle correlation is relatively flat and similar in magnitude to the azimuthal average of the di-jet signal, then the 3-particle cumulant cannot distinguish conical emission from other physics mechanisms. The 3-particle jet-like correlation, on the other hand, retains its discrimination power.

## 1. Introduction

Two-particle jet-like azimuthal correlations have revealed significant modification in central heavy-ion collisions at RHIC [1,2,3,4,5,6,7,8,9,10]. The away-side particles associated with and opposite to a high transverse momentum ( $p_T$ ) trigger particle were found to be broadly distributed at  $\Delta\phi = \pi$  in azimuth from the trigger particle, in contrast to observations from pp and d+Au collisions. The shape of the broad away-side distribution varies with the associated particle  $p_T$ . For  $1 < p_T < 2$  GeV/c, for instance, the away-side distribution may be even double-humped with a dip at  $\Delta\phi = \pi$  [2,3,4,5,6,7,8,9,10]. The away-side associated particles are also found to be not much harder than the bulk medium particles [2,3,4,5,7,8]; those at  $\Delta\phi = \pi$  are found to be softer than those in the angular regions where the humps appear [3,5,7,8], again in contrast to observations in pp and d+Au collisions or jet fragmentation in vacuum.

Several physical scenarios are possible to explain the observations. One is that jets may be deflected by radial transverse flow of the bulk medium or by the preferential selection of jet particles moving outwards than inwards due to energy loss [11]. Such a scenario would have jet particles narrowly clustered in individual events but the cluster is randomly distributed around  $\Delta\phi = \pi$  over many events. The second is large angle gluon radiation [12]. Such a scenario would have qualitatively similar structure as for deflected jets. The third is conical flow generated by sound shock-waves due to large energy deposition and perturbation by high momentum partons in the medium [13,14,15]. Such shock-waves result in a distinctive Mach-cone type structure where particles are preferentially emitted at a Mach angle determined by the speed of sound in the medium, independent of the particle  $p_T$ . If Mach-

cone type conical flow is indeed responsible for the observation, then the extraction of the speed of sound may be possible, thereby the equation of state of the created medium. The fourth is Cerenkov radiation generated by interactions of fast moving particles with the medium [16]. Such a scenario would have a similar structure as for the Mach-cone conical flow, but the Cerenkov angle will depend on the associated particle  $p_T$  [16].

Two-particle correlations cannot distinguish these scenarios because they give qualitatively the same 2-particle correlation. Such ambiguity is lifted in 3-particle correlation and its  $p_T$  dependence. If the broad 2-particle correlation is due to deflected jets or large angle gluon radiation, the two associated particles will be narrowly clustered in angle but the cluster will swing over a wide range in azimuth on the away side. If the Mach-cone or Cerenkov radiation is responsible for the broad 2-particle correlation, then the two associated particles will have equal probability being opposite away from  $\Delta\phi = \pi$  as being clustered together. A 3-particle correlation signal with opposite azimuthal angles from  $\Delta\phi = \pi$  for the two associated particles is, therefore, a distinctive signature of Mach-cone conical flow or Cerenkov radiation. The  $p_T$  dependence of the cone angle will further discriminate between the two scenarios of Mach-cone conical flow and Cerenkov gluon radiation [16].

Three-particle jet-like azimuthal correlations have been studied in STAR [7,8,17]. Recent high statistics results [17] have shown distinctive features of conical emission from Mach-cone and/or Cerenkov radiation. The analysis followed the jet-correlation method commonly used in 2-particle azimuthal correlation studies at RHIC [1,2,3,4,5,6,7,8,9,10], but extended to three particles. Hereon we will refer to this method as the *jet-correlation method*. Recently another analysis method, the 3-particle cumulant method [18], has been proposed. The method follows the mathematically well defined cumulant concept. Hereon we will refer to this method as the *cumulant method*. The two methods give different results and may confuse the general reader. In this paper we shall compare the two methods and discuss their differences in detail. We first give brief descriptions of the two methods. We then compare the two methods and discuss their differences, using a simple analytical model for jets. Finally we draw our conclusions.

## 2. Descriptions of the Two Analysis Methods

The objectives of the two analysis methods, the jet-correlation method and the cumulant method, are both to study jet structures. Due to the large particle multiplicity in relativistic heavy-ion collisions, event-by-event reconstruction of jets is impossible; one often resorts to 2- and 3-particle azimuthal correlations of charged hadrons with high  $p_T$  trigger particles that have a relatively large probability to originate from di-jets. The obtained correlation functions, thus, yield information on the di-jets. In this section, we briefly describe the two analysis methods for 3-particle azimuthal correlation studies.

### 2.1 The Cumulant Method

The 3-particle cumulant method is described in detail in [18]. Given a high  $p_T$  trigger particle to preferentially select a di-jet, the 2-particle cumulant is defined as

$$(1) \quad \hat{\rho}_2(\varphi_T, \varphi) = \rho_2(\varphi_T, \varphi) - \rho_1(\varphi_T)\rho_1(\varphi),$$

where  $\varphi_T$  and  $\varphi$  are the azimuthal angles of the trigger and associated particles, respectively. The 3-particle cumulant is defined as

$$(2) \quad \hat{\rho}_3(\varphi_T, \varphi_1, \varphi_2) = \rho_3(\varphi_T, \varphi_1, \varphi_2) - \rho_2(\varphi_T, \varphi_1)\rho_1(\varphi_2) - \rho_2(\varphi_T, \varphi_2)\rho_1(\varphi_1) - \rho_2(\varphi_1, \varphi_2)\rho_1(\varphi_T) + 2\rho_1(\varphi_T)\rho_1(\varphi_1)\rho_1(\varphi_2),$$

where  $\varphi_i$  is the azimuthal angle of the  $i^{\text{th}}$  associated particle ( $i=1,2$ ). In Eq.(2),  $\rho_1(\varphi) = dN/d\varphi$  is the single particle density and is constant (we shall just use  $\rho_1$ ),  $\rho_2(\varphi_1, \varphi_2) = d^2N/d\varphi_1d\varphi_2$  is the 2-particle density, and  $\rho_3(\varphi_T, \varphi_1, \varphi_2) = d^3N/d\varphi_Td\varphi_1d\varphi_2$  is the 3-particle density. Normalized per trigger particle, the 2-particle cumulant is

$$(3) \quad \hat{\rho}_2(\Delta\varphi) = \rho_2(\Delta\varphi) - \rho_1,$$

and the 3-particle cumulant is

$$(4a) \quad \hat{\rho}_3(\Delta\varphi_1, \Delta\varphi_2) = \rho_3(\Delta\varphi_1, \Delta\varphi_2) - \rho_2(\Delta\varphi_1)\rho_1 - \rho_2(\Delta\varphi_2)\rho_1 - \rho_2(\Delta\varphi_1, \Delta\varphi_2) + 2\rho_1^2,$$

Or alternatively

$$(4b) \quad \hat{\rho}_3(\Delta\varphi_1, \Delta\varphi_2) = \rho_3(\Delta\varphi_1, \Delta\varphi_2) - \hat{\rho}_2(\Delta\varphi_1)\rho_1 - \hat{\rho}_2(\Delta\varphi_2)\rho_1 - \rho_2(\Delta\varphi_1, \Delta\varphi_2).$$

In Eqs.(3), (4a) and (4b),  $\rho_2(\Delta\varphi) = dN/d\Delta\varphi$  is the 2-particle raw correlation function (or, equivalently, single-particle density of associated particles relative to the trigger particle azimuthal angle,  $\Delta\varphi = \varphi - \varphi_T$ ), and  $\rho_3(\Delta\varphi_1, \Delta\varphi_2) = d^3N/d\Delta\varphi_1d\Delta\varphi_2$  is the 3-particle raw correlation function (or, equivalently, pair-density of associated particle pairs relative to the trigger particle azimuthal angle,  $\Delta\varphi_i = \varphi_i - \varphi_T$ ). In addition,  $\rho_2(\Delta\varphi_1, \Delta\varphi_2) \equiv \rho_2(\varphi_1, \varphi_2) = d^2N/d\varphi_1d\varphi_2$  is the 2-particle density but expressed in terms of the azimuth differences of the particles from a random trigger particle.

The beauty of the cumulants is that they are mathematically well defined. The data analysis is straightforward. One calculates the cumulants for each event and accumulates them over events; the cumulants can be binned in fixed-multiplicity bins. The shortcoming, as we will see, is the difficulty in the interpretation of the obtained cumulants: the cumulants are mathematically well defined and thus do not depend on the underlying physics of the events, their interpretations, therefore, have to depend on the model for the underlying physics.

## 2.2 The Jet-Correlation Method

The 3-particle jet-correlation method is described in [7,8,17,19]. The method is extended from the commonly used 2-particle jet-correlation method to three particles. Combinatoric backgrounds are obtained from mixed-events technique; they include background from three “random” particles as well as background from a correlated trigger-associated particle pair with a “random” soft particle. The “random” particles we refer to here (and hereafter without the quotes) may include correlation due to anisotropic flow.

The jet-like correlation method has the jet model in mind. The difficulty is that the underlying background and the jet signal strength are unknown. One has to make an *ad hoc* working assumption about the background level. The common assumptions made in data analysis are ZYA1 [2,3,4,7,8,17,19] and ZYAM [4,6,9,10]. The correlation measured at RHIC is the lowest around  $\Delta\varphi = \pm 1$ . The STAR experiment makes the assumption that the jet signal is zero within the fixed range of  $0.8 < |\Delta\varphi| < 1.2$

(ZYA1) [2], while the PHENIX experiment uses the so-called Zero-Yield-At-Minimum (ZYAM) method in which the  $\Delta\phi$  region where the signal minimum resides is determined by the data itself [6].

The 2-particle jet-like correlation is

$$(5) \quad \hat{J}_2(\Delta\phi) = J_2(\Delta\phi) - B_2(\Delta\phi),$$

where  $J_2(\Delta\phi)$  is the 2-particle raw correlation function between the trigger and associated particles, and  $B_2(\Delta\phi)$  is the combinatoric background normalized by the aforementioned normalization schemes.

The 3-particle jet-like correlation is

$$(6a) \quad \hat{J}_3(\Delta\phi_1, \Delta\phi_2) = J_3(\Delta\phi_1, \Delta\phi_2) - \hat{J}_2(\Delta\phi_1)B_2(\Delta\phi_2) - \hat{J}_2(\Delta\phi_2)B_2(\Delta\phi_1) - B_3(\Delta\phi_1, \Delta\phi_2).$$

or alternatively

$$(6b) \quad \hat{J}_3(\Delta\phi_1, \Delta\phi_2) = J_3(\Delta\phi_1, \Delta\phi_2) - J_2(\Delta\phi_1)B_2(\Delta\phi_2) - J_2(\Delta\phi_2)B_2(\Delta\phi_1) - B_3(\Delta\phi_1, \Delta\phi_2) + 2B_2(\Delta\phi_1)B_2(\Delta\phi_2).$$

Here  $J_3(\Delta\phi_1, \Delta\phi_2)$  is the 3-particle raw correlation function, and  $B_3(\Delta\phi_1, \Delta\phi_2)$  is the combinatoric background of 3-particle correlation between two random background soft particles with a random trigger particle. The second and third terms in the r.h.s and Eqs.(6a) and (6b) are the hard-soft background, the combinatoric background of a correlated trigger-associated pair with a random background particle. It is given by folding the 2-particle jet-correlation signal  $\hat{J}_2$  with the underlying background  $B_2$ .

The advantage of the jet-correlation method is that, once the assumption about the background is made and the level of background is determined, the resultant 3-particle jet-like correlation results are easy to interpret and can be used to discriminate different physics scenarios. The disadvantage is of course the difficulty of the analysis.

### 3. Comparisons between the Two Methods

First we note that the raw 2- and 3-particle correlation functions in these two methods are identical, namely

$$(7a) \quad \rho_2(\Delta\phi) \equiv J_2(\Delta\phi),$$

$$(7b) \quad \rho_3(\Delta\phi_1, \Delta\phi_2) \equiv J_3(\Delta\phi_1, \Delta\phi_2).$$

Throughout this paper, we assume that no intrinsic correlations (except those due to anisotropic flow) exist between the two soft particles in the background. We shall first compare the two methods in a very simple case, in which the background particle distribution is uniform in azimuth relative to the trigger (i.e. no anisotropic flow). Such a comparison is enlightening as the difference between the two methods is straightforward and can be easily identified. We then include anisotropic flow in the comparison.

#### 3.1 Simple Case: Uniform Background

Since we consider no intrinsic correlation between the background soft particles and no anisotropic flow, we have

$$(8) \quad \rho_2(\Delta\varphi_1, \Delta\varphi_2) \equiv \rho_2(\varphi_1, \varphi_2) = \rho_1^2.$$

Here we have assumed that the number of pairs equals to the square of the number of particles, which is the case for Poisson or Gaussian multiplicity distributions. Using Eq.(8), Eq.(4a) and (4b) become

$$(9a) \quad \hat{\rho}_3(\Delta\varphi_1, \Delta\varphi_2) = \rho_3(\Delta\varphi_1, \Delta\varphi_2) - \rho_2(\Delta\varphi_1)\rho_1 - \rho_2(\Delta\varphi_2)\rho_1 + \rho_1^2,$$

$$(9b) \quad \hat{\rho}_3(\Delta\varphi_1, \Delta\varphi_2) = \rho_3(\Delta\varphi_1, \Delta\varphi_2) - \hat{\rho}_2(\Delta\varphi_1)\rho_1 - \hat{\rho}_2(\Delta\varphi_2)\rho_1 - \rho_1^2.$$

Since no anisotropic flow is considered, the background distribution in jet-correlation method is uniform,

$$(10a) \quad B_2(\Delta\varphi) = B_1,$$

where  $B_1$  is the average single particle density. Since we consider no intrinsic correlation between the two background particles, we have

$$(10b) \quad B_3(\Delta\varphi_1, \Delta\varphi_2) = B_1^2.$$

Thus Eqs.(6a) and (6b) become

$$(11a) \quad \hat{J}_3(\Delta\varphi_1, \Delta\varphi_2) = J_3(\Delta\varphi_1, \Delta\varphi_2) - \hat{J}_2(\Delta\varphi_1)B_1 - \hat{J}_2(\Delta\varphi_2)B_1 - B_1^2,$$

$$(11b) \quad \hat{J}_3(\Delta\varphi_1, \Delta\varphi_2) = J_3(\Delta\varphi_1, \Delta\varphi_2) - J_2(\Delta\varphi_1)B_1 - J_2(\Delta\varphi_2)B_1 + B_1^2.$$

The single particle densities in the two methods are different:  $\rho_1$  is larger than  $B_1$ , and

$$(12) \quad \rho_1 - B_1 = \langle \hat{J}_2 \rangle$$

where  $\langle \hat{J}_2 \rangle$  is the average associated particle multiplicity density in azimuth. As we shall see, this difference is the essential piece that makes the results from the two methods different.

Using Eqs.(7), (5), (10a) and (12), the difference between the 3-particle cumulant, Eq.(9a), and the 3-particle jet-correlation, Eq.(11b), is given by

$$(13) \quad \Delta = \hat{\rho}_3(\Delta\varphi_1, \Delta\varphi_2) - \hat{J}_3(\Delta\varphi_1, \Delta\varphi_2) = -\langle \hat{J}_2 \rangle \left[ \hat{J}_2(\Delta\varphi_1) + \hat{J}_2(\Delta\varphi_2) - \langle \hat{J}_2 \rangle \right].$$

To give further insights, we consider the simple case in which the 3-particle jet-correlation function is simply the product of the two 2-particle jet-correlation functions (i.e. the 3-particle jet-correlation function is factorized):

$$(14) \quad \hat{J}_3(\Delta\varphi_1, \Delta\varphi_2) = \hat{J}_2(\Delta\varphi_1)\hat{J}_2(\Delta\varphi_2).$$

Then, using Eq.(13), the 3-particle cumulant is simply

$$(15) \quad \hat{\rho}_3(\Delta\varphi_1, \Delta\varphi_2) = \left[ \hat{J}_2(\Delta\varphi_1) - \langle \hat{J}_2 \rangle \right] \left[ \hat{J}_2(\Delta\varphi_2) - \langle \hat{J}_2 \rangle \right].$$

This should come as no surprise; the 3-particle cumulant can also be factorized into two 2-particle cumulants that are given by Eq.(3). The difference between the two methods is in the background level. The jet-correlation method puts the background at ZYA1 or ZYAM, and the cumulant method, by definition, effectively takes the average of the correlation signal as background. In fact, if the jet-correlation method also takes the average as the background, i.e. the 2-particle jet-correlation signal is now  $\hat{J}_2(\Delta\varphi) - \langle \hat{J}_2 \rangle$  instead of  $\hat{J}_2(\Delta\varphi)$ , then it will yield the identical result as that from the cumulant method in Eq.(15).

To give a visual comparison between the two methods, we use a specific example. We define a jet-like 2-particle correlation with a near side peak and a broad double-hump away-side distribution:

$$(16) \quad \hat{J}_2(\Delta\varphi) = \frac{N_1}{\sqrt{2\pi}\sigma_1} \exp\left[-\frac{(\Delta\varphi)^2}{2\sigma_1^2}\right] + \frac{N_2/2}{\sqrt{2\pi}\sigma_2} \left( \exp\left[-\frac{(\Delta\varphi + \alpha)^2}{2\sigma_2^2}\right] + \exp\left[-\frac{(\Delta\varphi - \alpha)^2}{2\sigma_2^2}\right] \right).$$

We suppose this jet-like 2-particle correlation is present in every event (i.e. Mach-cone event), and it is sitting on a large flat background,  $B_{true} = 150/2\pi$ . We take the Mach-cone angle to be  $\alpha = 1$ . We study two cases of jet signals: (A) In the first case, the jets are narrow with  $\sigma_1 = 0.2$  and  $\sigma_2 = 0.2$ . (B) In the second case, we use a realistic jet signal as measured in experiment [3,5,7,8,17], with  $\sigma_1 = 0.4$  and  $\sigma_2 = 0.7$ . For both cases, we take the numbers of associated particles to be  $N_1 = 0.7$  and  $N_2 = 1.2$ , respectively for near side and away side. These numbers are chosen so that the 2-particle jet-correlation signal in the second case corresponds, qualitatively, to the measured one [3,5,7,8,17]. For both cases the minimum signal strength is at  $\Delta\varphi \approx 1$ ; for case (A) the normalized background level is  $B_1 \approx B_{true}$ , and for case (B) the normalized background is  $B_1 \approx B_{true} + 0.12$ . For easy reference, we list the parameters below:

(17A) Narrow jets:  $N_1 = 0.7, N_2 = 1.2, \sigma_1 = 0.2, \sigma_2 = 0.2, \alpha = 1; B_{true} = 150/2\pi, B_1 = B_{true}$ .

(17B) Realistic jets:  $N_1 = 0.7, N_2 = 1.2, \sigma_1 = 0.4, \sigma_2 = 0.7, \alpha = 1; B_{true} = 150/2\pi, B_1 = B_{true} + 0.12$ .

We assume that the 3-particle jet-like correlation can be factorized as the product of the two 2-particle jet-like correlation functions given by Eq.(14). In other words, the two soft particles are not intrinsically correlated, but are correlated due to their individual correlations to the same trigger particle. This corresponds to the following extreme jet fragmentation scenario: the trigger particle direction is the jet axis, and fragmentations into individual hadrons are identical and independent of each other.

The raw 3-particle correlation is then given by

$$(18) \quad J_3(\Delta\varphi_1, \Delta\varphi_2) = \hat{J}_2(\Delta\varphi_1)\hat{J}_2(\Delta\varphi_2) + \hat{J}_2(\Delta\varphi_1)B_{true} + \hat{J}_2(\Delta\varphi_2)B_{true} + B_{true}^2 = \left[ \hat{J}_2(\Delta\varphi_1) + B_{true} \right] \left[ \hat{J}_2(\Delta\varphi_2) + B_{true} \right].$$

This raw 3-particle correlation is needed as the starting point of any data analysis. One can extract the 3-particle jet-correlation from the raw signal by taking different assumptions of the underlying background level, which is the essential difference between the jet-correlation and the cumulant methods.

The raw 2-particle correlation is shown in Figure 1(a) for case (A). The blue line shows the real background level,  $B_{true}$ , (or the normalized background level  $B_1$ , which equals to  $B_{true}$ ). The red line shows the single particle density,  $\rho_1$ , used in the cumulant method. The 3-particle correlation signal after subtraction of the real background level (i.e.  $B_{true}$ ) is shown in Figure 1(b). This is the genuine 3-particle correlation function that was initially put in, which shows the distinctive Mach-cone structure. The 3-particle cumulant result is shown in Figure 1(c). This is equivalent to what the 3-particle jet-correlation analysis would result by subtracting an overestimated background level of  $B_1 = \rho_1$ , given by Eq.(15) where  $\langle \hat{J}_2 \rangle = \rho_1 - B_{true}$ . The Mach-cone structure is partially preserved in the 3-particle cumulant result. The negative strips are produced by the over-subtraction of the average signal particle density, which is larger than the true background level.

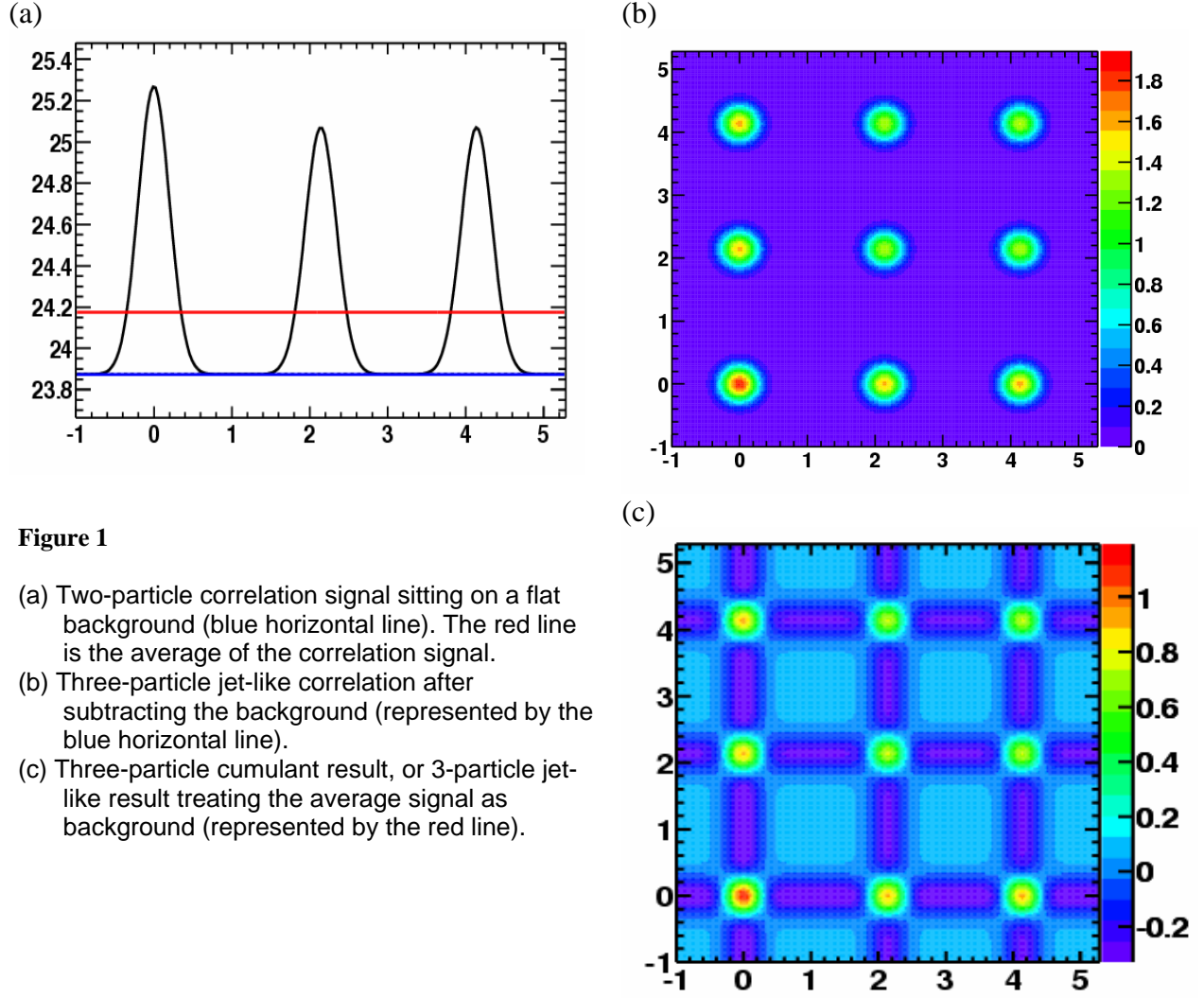


**Figure 1**

- (a) Two-particle correlation signal sitting on a flat background (blue horizontal line). The red line is the average of the correlation signal.
- (b) Three-particle jet-like correlation after subtracting the background (represented by the blue horizontal line).
- (c) Three-particle cumulant result, or 3-particle jet-like result treating the average signal as background (represented by the red line).

The raw 2-particle correlation for case (B) is shown in Figure 2(a). The black line shows the real background level  $B_{true}$ . The blue line shows the normalized background level  $B_1$ , such that the jet signal is zero at minimum. The red line shows the single particle density,  $\rho_1$ , used in the cumulant method. The 3-particle jet-correlation signal after subtraction of the real background level (i.e.  $B_{true}$ ) is shown in Figure 2(b). Again, this is the genuine 3-particle jet-correlation function that was initially put in,  $\hat{J}_3(\Delta\phi_1, \Delta\phi_2) = \hat{J}_2(\Delta\phi_1)\hat{J}_2(\Delta\phi_2)$ . The 3-particle jet-correlation signal after subtraction of the normalized background level (i.e.  $B_1$ ) is shown in Figure 2(c). This would be the 3-particle jet-correlation function from data analysis using ZYA1 or ZYAM background normalization scheme. Since the background is overestimated, the obtained 3-particle jet-correlation signal is lower than the true signal, but the structure of the genuine 3-particle jet-correlation (i.e. the Mach-cone structure) is preserved. In fact, the 3-particle jet-correlation signal with the overestimated background,  $B_1 > B_{true}$ , is given by

$$(19) \quad \hat{J}_3(\Delta\phi_1, \Delta\phi_2) = \left[ \hat{J}_2(\Delta\phi_1) - \delta B \right] \left[ \hat{J}_2(\Delta\phi_2) - \delta B \right] \quad \text{where } \delta B = B_1 - B_{true}.$$

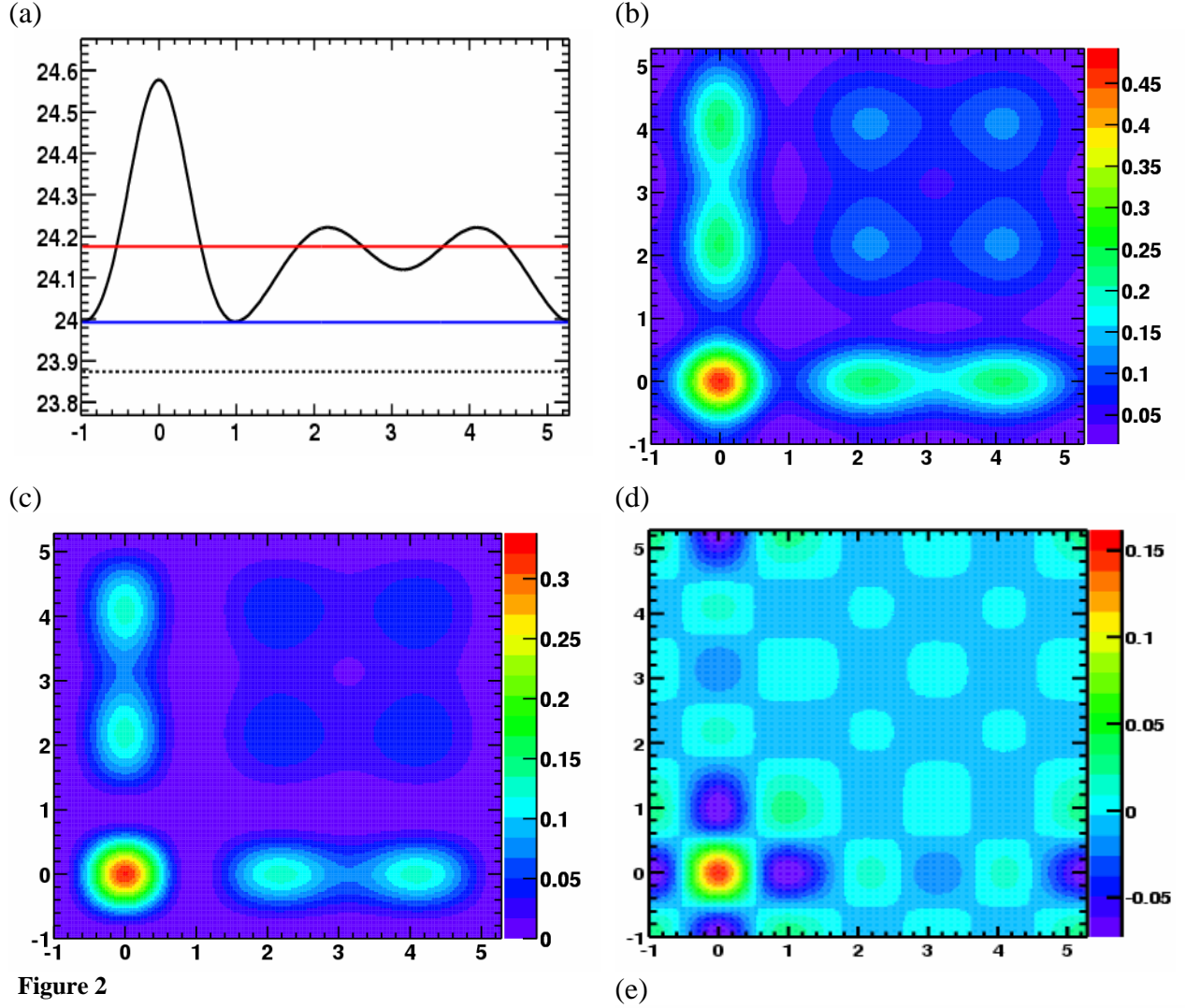


Figure 2

- (a) Two-particle correlation signal sitting on a flat background (black horizontal line). The blue line is the overestimated background level to match the signal at the minimum. The red line is the average of the correlation signal.
- (b) Three-particle jet-like correlation after subtracting the true background (represented by the black horizontal line).
- (c) Three-particle jet-like correlation with background normalized to the signal at  $\Delta\phi = 1$  (represented by the blue line). Note the Mach-cone structure is still present.
- (d) Three-particle cumulant result, or 3-particle jet-like result treating the average signal as background (represented by the red line).
- (e) Zoomed version of the plot in (d).



Figure 2(d) shows the 3-particle cumulant result. The structure of the cumulant result is quite complicated and different from the 3-particle jet-correlation result. This is due to the subtraction of the average single particle density, which is larger than the true background level. Unlike the simple case (A) where the jet peaks are narrow and well-confined, the broad jet peaks and the over-subtraction of the background level in case (B) create the complicated structure in the cumulant result. The distinctive Mach-cone structure on the away-side that is initially put in is hardly observable in the cumulant result. This is because the away-side 2-particle correlation as shown in Figure 2(a), qualitatively similar to that measured in real data [3,5,7,8,17], is quite flat and happens to have similar magnitude as the average single particle density. After subtraction of the single particle density, the away-side 2-particle correlation strength is more or less subtracted away and can hardly show up in the final 3-particle cumulant. Figure 2(e) shows the zoomed-in plot of the cumulant result in Figure 2(d). The structure due to the double-hump in the away-side 2-particle correlation, which resembles the Mach-cone structure, is visible on this fine level of the current analytical demonstration of the cumulant result. However, it would be hard to observe in a real data analysis due to the other present complicated structures and limited statistics.

### 3.2 Background with Anisotropic Flow

In heavy-ion collisions, the background particles are correlated to the reaction plane due to the hydrodynamic type of collective flow of the bulk medium and the anisotropic overlap region between the colliding nuclei. The trigger particle emission is also correlated to the reaction plane due to, not so much of the hydrodynamic type collective flow, but the path-length dependent energy loss of high  $p_T$  particles in the medium that is initially anisotropic. This reaction plane correlation, expressed in harmonics up to the fourth order, is given by

$$(20) \quad B_2(\Delta\varphi) = B_1 \left[ 1 + 2v_2^{trig} v_2 \cos 2(\Delta\varphi) + 2v_4^{trig} v_4 \cos 4(\Delta\varphi) \right],$$

where  $v_2^{trig}$  and  $v_2$  are the elliptic flow of the trigger and associated particles, respectively. Likewise  $v_4^{trig}$  and  $v_4$  are the respective fourth harmonic coefficients. The 2-particle jet-correlation signal of Eq.(5) is then,

$$(21) \quad \hat{J}_2(\Delta\varphi) = J_2(\Delta\varphi) - B_1 \left[ 1 + 2v_2^{trig} v_2 \cos 2(\Delta\varphi) + 2v_4^{trig} v_4 \cos 4(\Delta\varphi) \right].$$

There are two combinatoric backgrounds to 3-particle jet-correlation. One is that of a correlated trigger-associated pair combined with a random background particle. This hard-soft background can be obtained by folding the 2-particle jet-correlation signal with the underlying background particle, namely  $\hat{J}_2(\Delta\varphi_1)B_2(\Delta\varphi_2) + \hat{J}_2(\Delta\varphi_2)B_2(\Delta\varphi_1)$ . The other combinatoric background is due to the trigger particle combined with two random particles from the underlying background. This soft-soft background term normalized per trigger particle, considering only the anisotropic flow correlation, is given by [19]

$$(22) \quad B_3(\Delta\varphi_1, \Delta\varphi_2) = B_1^2 \left( \begin{aligned} &1 + 2v_2^{trig} v_2^{(1)} \cos 2(\Delta\varphi_1) + 2v_2^{trig} v_2^{(2)} \cos 2(\Delta\varphi_2) + 2v_2^{(1)} v_2^{(2)} \cos 2(\Delta\varphi_1 - \Delta\varphi_2) \\ &+ 2v_4^{trig} v_4^{(1)} \cos 4(\Delta\varphi_1) + 2v_4^{trig} v_4^{(2)} \cos 4(\Delta\varphi_2) + 2v_4^{(1)} v_4^{(2)} \cos 4(\Delta\varphi_1 - \Delta\varphi_2) \\ &+ 2v_2^{trig} v_2^{(1)} v_4^{(2)} \cos 2(\Delta\varphi_1 - 2\Delta\varphi_2) + 2v_2^{trig} v_2^{(2)} v_4^{(1)} \cos 2(2\Delta\varphi_1 - \Delta\varphi_2) + 2v_2^{(1)} v_2^{(2)} v_4^{trig} \cos 2(\Delta\varphi_1 + \Delta\varphi_2) \end{aligned} \right).$$

We note that in real collision data the background particles have not only anisotropic flow correlation, but also other correlations that are unrelated to the trigger particle, such as jet-correlations due to jets

other than the one selected by the trigger particle [20]. We do not consider these correlations in this paper because they are not important for the purpose of our study.

The final 3-particle jet-correlation function is given by

$$(23a) \quad \hat{J}_3(\Delta\varphi_1, \Delta\varphi_2) = J_3(\Delta\varphi_1, \Delta\varphi_2) - \hat{J}_2(\Delta\varphi_1)B_2(\Delta\varphi_2) - \hat{J}_2(\Delta\varphi_2)B_2(\Delta\varphi_1) - B_3(\Delta\varphi_1, \Delta\varphi_2),$$

or alternatively

$$(23b) \quad \hat{J}_3(\Delta\varphi_1, \Delta\varphi_2) = J_3(\Delta\varphi_1, \Delta\varphi_2) - J_2(\Delta\varphi_1)B_2(\Delta\varphi_2) - J_2(\Delta\varphi_2)B_2(\Delta\varphi_1) - B_3(\Delta\varphi_1, \Delta\varphi_2) + 2B_2(\Delta\varphi_1)B_2(\Delta\varphi_2).$$

It is interesting to consider only anisotropic flow correlation, no jet-like correlation. Obviously, if no jet-like correlation is present, the 3-particle jet-correlation will give zero signal as there will be no 2-particle jet-correlation signal to start with,  $\hat{J}_2(\Delta\varphi) = 0$ . However, the 3-particle cumulant will still yield non-zero result, as we demonstrate below.

With only anisotropic flow correlation present, the raw 1-, 2- and 3-particle cumulants are simply given by the background,  $\rho_1 = B_1$ ,  $\rho_2(\Delta\varphi) = B_2(\Delta\varphi)$  and  $\rho_3(\Delta\varphi_1, \Delta\varphi_2) = B_3(\Delta\varphi_1, \Delta\varphi_2)$ . Thus the 3-particle cumulant from Eq.(4a) is

$$(24) \quad \hat{\rho}_3(\Delta\varphi_1, \Delta\varphi_2) = B_3(\Delta\varphi_1, \Delta\varphi_2) - B_2(\Delta\varphi_1)B_1 - B_2(\Delta\varphi_2)B_1 - B_2(\Delta\varphi_1 - \Delta\varphi_2) + 2B_1^2.$$

Here  $B_2(\Delta\varphi)$  is given by Eq.(20),  $B_3(\Delta\varphi_1, \Delta\varphi_2)$  by Eq.(22), and  $B_2(\Delta\varphi_1 - \Delta\varphi_2)$  is the 2-particle correlation between the two soft particles normalized per trigger particle, and is given by

$$(25) \quad B_2(\Delta\varphi_1 - \Delta\varphi_2) = B_1^2 \left[ 1 + 2v_2^2 \cos 2(\Delta\varphi_1 - \Delta\varphi_2) + 2v_4^2 \cos 4(\Delta\varphi_1 - \Delta\varphi_2) \right].$$

With simple algebra, we obtain

$$(26) \quad \hat{\rho}_3(\Delta\varphi_1, \Delta\varphi_2) = 2B_1^2 \left[ v_2^{trig} v_2^{(1)} v_4^{(2)} \cos 2(\Delta\varphi_1 - 2\Delta\varphi_2) + v_2^{trig} v_2^{(2)} v_4^{(1)} \cos 2(2\Delta\varphi_1 - \Delta\varphi_2) + v_2^{(1)} v_2^{(2)} v_4^{trig} \cos 2(\Delta\varphi_1 + \Delta\varphi_2) \right].$$

So with no jet correlation, only anisotropic flow correlation present, the 3-particle cumulant gives non-zero correlation result. This shows that the 3-particle cumulant measures something different from simple jet-correlation; it measures 3-particle correlation regardless of the nature of the underlying physics. Although the result in Eq.(26) is on the order of  $v_2^4$ , its magnitude can be still sizeable due to the large background level of  $B_1^2$  in relativistic heavy-ion collisions.

Now we turn our attention to the realistic situation where both jet-correlation and anisotropic flow correlation are present, and compare the results from the two methods. From Eqs.(4a),(7),(12), and using

$$(27) \quad \rho_2(\Delta\varphi_1, \Delta\varphi_2) = \rho_1^2 \left[ 1 + 2v_2^2 \cos 2(\Delta\varphi_1 - \Delta\varphi_2) + 2v_4^2 \cos 4(\Delta\varphi_1 - \Delta\varphi_2) \right] = (\rho_1 / B_1)^2 B_2(\Delta\varphi_1 - \Delta\varphi_2),$$

we obtain

$$(28) \quad \hat{\rho}_3(\Delta\varphi_1, \Delta\varphi_2) = J_3(\Delta\varphi_1, \Delta\varphi_2) - J_2(\Delta\varphi_1) \left( B_1 + \langle \hat{J}_2 \rangle \right) - J_2(\Delta\varphi_2) \left( B_1 + \langle \hat{J}_2 \rangle \right) - \left( 1 + \langle \hat{J}_2 \rangle / B_1 \right)^2 B_2(\Delta\varphi_1 - \Delta\varphi_2) + 2 \left( B_1 + \langle \hat{J}_2 \rangle \right)^2.$$

Taking the difference between Eq.(28) and Eq.(6b), using Eqs.(22) and (25), we have

$$\begin{aligned}
\Delta &= \hat{\rho}_3(\Delta\varphi_1, \Delta\varphi_2) - \hat{J}_3(\Delta\varphi_1, \Delta\varphi_2) \\
&= J_2(\Delta\varphi_1) \left( B_1 \left[ 1 + 2v_2^{trig} v_2^{(2)} \cos 2(\Delta\varphi_2) + 2v_4^{trig} v_4^{(2)} \cos 4(\Delta\varphi_2) \right] - B_1 - \langle \hat{J}_2 \rangle \right) \\
&\quad + J_2(\Delta\varphi_2) \left( B_1 \left[ 1 + 2v_2^{trig} v_2^{(1)} \cos 2(\Delta\varphi_1) + 2v_4^{trig} v_4^{(1)} \cos 4(\Delta\varphi_1) \right] - B_1 - \langle \hat{J}_2 \rangle \right) \\
(29) \quad &\quad + B_1^2 \left( \begin{aligned} &1 + 2v_2^{trig} v_2^{(1)} \cos 2(\Delta\varphi_1) + 2v_2^{trig} v_2^{(2)} \cos 2(\Delta\varphi_2) + 2v_2^{(1)} v_2^{(2)} \cos 2(\Delta\varphi_1 - \Delta\varphi_2) \\ &+ 2v_4^{trig} v_4^{(1)} \cos 4(\Delta\varphi_1) + 2v_4^{trig} v_4^{(2)} \cos 4(\Delta\varphi_2) + 2v_4^{(1)} v_4^{(2)} \cos 4(\Delta\varphi_1 - \Delta\varphi_2) \\ &+ 2v_2^{trig} v_2^{(1)} v_4^{(2)} \cos 2(\Delta\varphi_1 - 2\Delta\varphi_2) + 2v_2^{trig} v_2^{(2)} v_4^{(1)} \cos 2(2\Delta\varphi_1 - \Delta\varphi_2) + 2v_2^{(1)} v_2^{(2)} v_4^{trig} \cos 2(\Delta\varphi_1 + \Delta\varphi_2) \end{aligned} \right) \\
&\quad - \left( B_1^2 + 2B_1 \langle \hat{J}_2 \rangle + \langle \hat{J}_2 \rangle^2 \right) \left[ 1 + 2v_2^{(1)} v_2^{(2)} \cos 2(\Delta\varphi_1 - \Delta\varphi_2) + 2v_4^{(1)} v_4^{(2)} \cos 4(\Delta\varphi_1 - \Delta\varphi_2) \right] + 2 \left( B_1^2 + 2B_1 \langle \hat{J}_2 \rangle + \langle \hat{J}_2 \rangle^2 \right) \\
&\quad - 2B_1^2 \left[ 1 + 2v_2^{trig} v_2^{(1)} \cos 2(\Delta\varphi_1) + 2v_4^{trig} v_4^{(1)} \cos 4(\Delta\varphi_1) \right] \left[ 1 + 2v_2^{trig} v_2^{(2)} \cos 2(\Delta\varphi_2) + 2v_4^{trig} v_4^{(2)} \cos 4(\Delta\varphi_2) \right].
\end{aligned}$$

After simple algebra, we arrive at

$$\begin{aligned}
\Delta &= -\langle \hat{J}_2 \rangle \left( \hat{J}_2(\Delta\varphi_1) + \hat{J}_2(\Delta\varphi_2) - \langle \hat{J}_2 \rangle \right) \\
&\quad + B_1 \left( \hat{J}_2(\Delta\varphi_1) - \langle \hat{J}_2 \rangle \right) \left[ 2v_2^{trig} v_2^{(2)} \cos 2(\Delta\varphi_2) + 2v_4^{trig} v_4^{(2)} \cos 4(\Delta\varphi_2) \right] \\
(30) \quad &\quad + B_1 \left( \hat{J}_2(\Delta\varphi_2) - \langle \hat{J}_2 \rangle \right) \left[ 2v_2^{trig} v_2^{(1)} \cos 2(\Delta\varphi_1) + 2v_4^{trig} v_4^{(1)} \cos 4(\Delta\varphi_1) \right] \\
&\quad - \langle \hat{J}_2 \rangle \left( 2B_1 + \langle \hat{J}_2 \rangle \right) \left[ 2v_2^{(1)} v_2^{(2)} \cos 2(\Delta\varphi_1 - \Delta\varphi_2) + 2v_4^{(1)} v_4^{(2)} \cos 4(\Delta\varphi_1 - \Delta\varphi_2) \right] \\
&\quad + B_1^2 \left[ 2v_2^{trig} v_2^{(1)} v_4^{(2)} \cos 2(\Delta\varphi_1 - 2\Delta\varphi_2) + 2v_2^{trig} v_2^{(2)} v_4^{(1)} \cos 2(2\Delta\varphi_1 - \Delta\varphi_2) + 2v_2^{(1)} v_2^{(2)} v_4^{trig} \cos 2(\Delta\varphi_1 + \Delta\varphi_2) \right].
\end{aligned}$$

The 3-particle cumulant is therefore

$$\begin{aligned}
\hat{\rho}_3(\Delta\varphi_1, \Delta\varphi_2) &= \left[ \hat{J}_2(\Delta\varphi_1) - \langle \hat{J}_2 \rangle \right] \left[ \hat{J}_2(\Delta\varphi_2) - \langle \hat{J}_2 \rangle \right] \\
(31) \quad &\quad + B_1 \left( \hat{J}_2(\Delta\varphi_1) - \langle \hat{J}_2 \rangle \right) \left[ 2v_2^{trig} v_2^{(2)} \cos 2(\Delta\varphi_2) + 2v_4^{trig} v_4^{(2)} \cos 4(\Delta\varphi_2) \right] \\
&\quad + B_1 \left( \hat{J}_2(\Delta\varphi_2) - \langle \hat{J}_2 \rangle \right) \left[ 2v_2^{trig} v_2^{(1)} \cos 2(\Delta\varphi_1) + 2v_4^{trig} v_4^{(1)} \cos 4(\Delta\varphi_1) \right] \\
&\quad - \langle \hat{J}_2 \rangle \left( 2B_1 + \langle \hat{J}_2 \rangle \right) \left[ 2v_2^{(1)} v_2^{(2)} \cos 2(\Delta\varphi_1 - \Delta\varphi_2) + 2v_4^{(1)} v_4^{(2)} \cos 4(\Delta\varphi_1 - \Delta\varphi_2) \right] \\
&\quad + B_1^2 \left[ 2v_2^{trig} v_2^{(1)} v_4^{(2)} \cos 2(\Delta\varphi_1 - 2\Delta\varphi_2) + 2v_2^{trig} v_2^{(2)} v_4^{(1)} \cos 2(2\Delta\varphi_1 - \Delta\varphi_2) + 2v_2^{(1)} v_2^{(2)} v_4^{trig} \cos 2(\Delta\varphi_1 + \Delta\varphi_2) \right].
\end{aligned}$$

The first line in the r.h.s. of Eq.(31) is the 3-particle cumulant result for the case of no anisotropic flow correlation, and the fifth line is the 3-particle cumulant due to anisotropic flow correlation as given by Eq.(26) for the case of no jet-correlation. However, there are additional terms in the rest of the r.h.s of Eq.(31), which arise from the coupling between jet-correlation and anisotropic flow correlation.

To give a visual impression of the 3-particle cumulant in Eq.(31), we use the jet-model of case (B) in Eq.(17B), but with additional anisotropic flow of magnitudes of  $v_2^{trig} = 7.5\%$ ,  $v_2^{(1)} = v_2^{(2)} = 5\%$ , and  $v_4 = v_2^2$ . Namely,

$$(32) \quad \begin{cases} N_1 = 0.7, N_2 = 1.2, \sigma_1 = 0.4, \sigma_2 = 0.7, \alpha = 1; \\ B_1 = B_{true} = 150/2\pi; v_2^{trig} = 0.075, v_2^{(1)} = v_2^{(2)} = 0.05, v_4 = v_2^2. \end{cases}$$

Note we have used  $B_1 = B_{true}$ , as the 2-particle jet-correlation  $\hat{J}_2(\Delta\varphi)$  we will use is not renormalized by ZYA1 or ZYAM. The 3-particle cumulant result will be the same if we use the 2-particle jet-correlation with normalized background and the corresponding new background level.

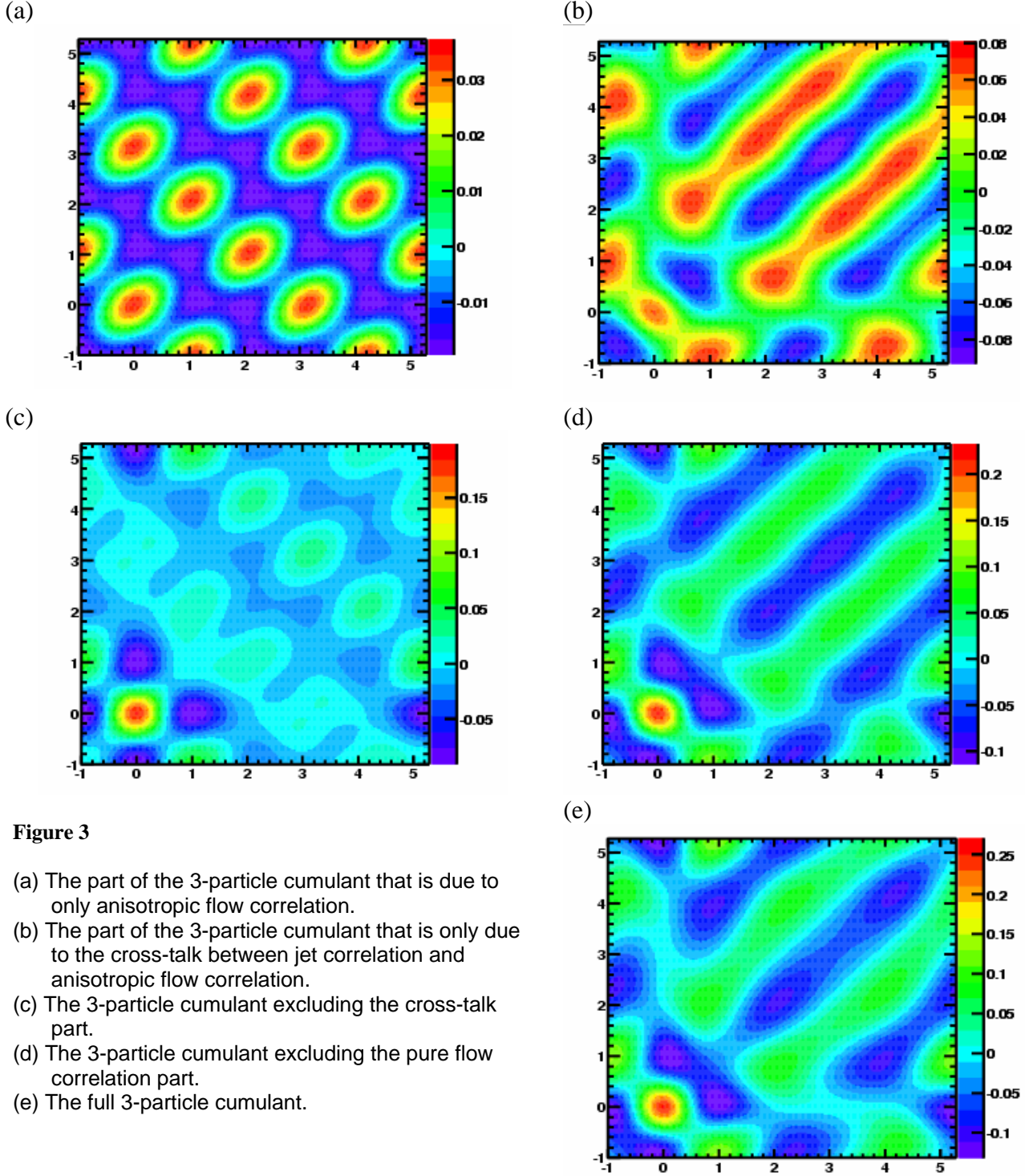


**Figure 3**

- (a) The part of the 3-particle cumulant that is due to only anisotropic flow correlation.
- (b) The part of the 3-particle cumulant that is only due to the cross-talk between jet correlation and anisotropic flow correlation.
- (c) The 3-particle cumulant excluding the cross-talk part.
- (d) The 3-particle cumulant excluding the pure flow correlation part.
- (e) The full 3-particle cumulant.

The jet-like correlation part of the 3-particle cumulant (but with over-subtraction of the background) is already shown in Figure 2(d) and (e). The part of the 3-particle cumulant due to only the anisotropic flow correlation by Eq.(26) is shown in Figure 3(a). The part due the cross-talk between jet-correlation and anisotropic flow correlation is shown in Figure 3(b). The 3-particle cumulant excluding the cross-talk part is shown in Figure 3(c). Likewise, The 3-particle cumulant excluding the pure flow

correlation part is shown in Figure 3(d). The full 3-particle cumulant as given by Eq.(31) is shown in Figure 3(e). The 3-particle cumulant result is very different from the 3-particle jet-correlation results shown in Figure 2(b) or (c).

## 4. Summary

We have described two analysis methods for 3-particle azimuthal correlations between a high transverse momentum trigger particle and two softer particles: the 3-particle *jet-correlation method* and the 3-particle *cumulant method*. We have compared the two methods analytically and analyzed their differences for two cases: one with a uniform background in azimuth and the other with a background including anisotropic flow. The major conclusions from our study are as follow:

- (1) The jet-correlation method has the jet-model in mind and is designed to study jet-like correlations; its interpretation is straightforward. The cumulant method does not have a particular correlation model in mind and is designed to study any kinds of correlations; its interpretation is, however, difficult and has to involve a correlation model.
- (2) The main difference between the two methods lies in the different background subtraction schemes.
- (3) For narrow jet peaks, both methods can identify Mach-cone structures, although the magnitudes and shapes of the correlation functions are different. For fat and more or less flat 2-particle jet-correlations on the away side, as measured in RHIC experiments, the jet-correlation method can still identify Mach-cone structures, while the cumulant method fails.

## Acknowledgements

We thank our STAR collaborators, in particular, Dr. Marco van Leeuwen, Dr. Claude Pruneau, and Dr. Sergei Voloshin for valuable discussions. This work is supported by U.S. Department of Energy under Grants DE-FG02-02ER41219 and DE-FG02-88ER40412.

## References:

- 
- [1] C. Adler *et al.* (STAR Collaboration), Phys. Rev. Lett. **90**, 082302 (2003) [nucl-ex/0210033].
  - [2] J. Adams *et al.* (STAR Collaboration), Phys. Rev. Lett. **95**, 152301 (2005) [nucl-ex/0501016].
  - [3] F. Wang (STAR Collaboration), Proceedings of RIKEN BNL Research Center Workshop “Jet Correlations at RHIC”, BNL, March 10-11, 2005.
  - [4] W. Holtzman (PHENIX Collaboration), Proceedings of RIKEN BNL Research Center Workshop “Jet Correlations at RHIC”, BNL, March 10-11, 2005.
  - [5] F. Wang, J. Phys. Conf. Ser. **27**, 32 (2005) [nucl-ex/0508021].
  - [6] S.S. Adler *et al.* (PHENIX Collaboration), Phys. Rev. Lett. **97**, 052301 (2006) [nucl-ex/0507004].
  - [7] J.G. Ulery (STAR Collaboration), nucl-ex/0510055.
  - [8] F. Wang (STAR Collaboration), nucl-ex/0510068.
  - [9] Y. Akiba (PHENIX Collaboration), Nucl. Phys. **A774**, 403 (2006) [nucl-ex/0510008].
  - [10] B. Cole, presentation at Quark Matter 2005.
  - [11] R. Hwa, presentation at Hard Probes 2006.
  - [12] I. Vitev, Phys. Lett. B **630**, **78** (2005) [hep-ph/0501255].
  - [13] H. Stoecker, Nucl. Phys. **A750**, 121 (2005) [nucl-th/0406018].
  - [14] Casalderrey-Solana, Shuryak, Teaney, J. Phys. Conf. Ser. **27**, 22 (2005) [hep-ph/0411315].

- 
- [15] Muller, Ruppert, nucl-th/0507043.
  - [16] Majumder, Phys. Rev. Lett. **96**, 172302 (2006) [nucl-th/0507063].
  - [17] J.G. Ulery (STAR Collaboration), presentation at Hard Probes 2006.
  - [18] C. Pruneau, nucl-ex/0608002.
  - [19] J.G. Ulery and F. Wang, nucl-ex/0609016.
  - [20] J. Adams *et al.* (STAR Collaboration), Phys. Rev. C **73**, 064907 (2006) [nucl-ex/0411003].